Journal of Environmental Management 361 (2024) 121242

Contents lists available at ScienceDirect

Journal of Environmental Management

journal homepage: www.elsevier.com/locate/jenvman

Research article

Growth and cooling potential of urban trees across different levels of imperviousness

Nayanesh Pattnaik [a,*], Martin Honold [b], Eleonora Franceschi [b], Astrid Moser-Reischl [a,b], Thomas Rötzer [b], Hans Pretzsch [b,c], Stephan Pauleit [a], Mohammad A. Rahman [a,d]

[a] Strategic Landscape Planning and Management, School of Life Sciences, Technical University of Munich, Emil-Ramann-Str. 6, 85354, Freising, Germany
[b] Forest Growth and Yield Science, School of Life Sciences, Technical University of Munich, Hans-Carl-von-Carlowitz-Platz 2, 85354, Freising, Germany
[c] Sustainable Forest Management Research Institute IuFOR, University Valladolid, Spain
[d] The University of Melbourne, Burnley, Victoria, Australia

ARTICLE INFO

Handling Editor: Jason Michael Evans

1. Introduction

City centers experience higher temperatures than surrounding suburban and rural areas due to the urban heat island effect (UHI) (Oke, 1988). Previous studies have observed localized hot and cool spots, large intra-urban temperature differences, and variations of UHI intensity within the city's boundaries (Buyantuyev and Wu, 2010; Heusinkveld et al., 2014). These variations are directly linked to various urban factors, such as land cover, surface characteristics, building size and shape, material properties, anthropogenic heat generated from vehicles, building systems, and industrial activities (Smithers et al., 2018). The primary cause of UHI is the modification in the surface energy balance due to changes in land cover types in urban areas (Oke, 1973). Coupled with climate change, UHI poses a serious threat to the quality of life of the population in urban areas (Iungman et al., 2023). Thus, implementing effective urban heat mitigation strategies is essential for to promote the adaptive capacity of our cities (Pauleit et al., 2020).

Cooler spots within the urban environment are positively correlated with greenspace and increased vegetation cover (Livesley et al., 2016). Therefore, urban green infrastructure (UGI), an interconnected network of strategically planned green spaces, is key in mitigating UHI (Pauleit et al., 2011). Within UGI, particular emphasis has been placed on trees' ability to reduce local heat stress through shading and evapotranspiration (Endreny et al., 2017; Gill et al., 2007; Livesley et al., 2016). Previous studies have shown that tree canopies restrict the amount of short-wave radiation reaching the surface by 60%–90%, which in turn reduces the surface temperatures between sunny asphalt areas and shaded areas by up to 40 °C (Armson et al., 2012; Rahman et al., 2020b). The process of transpiration releases water vapor into the surrounding atmosphere, which raises air humidity, but cools the local environment by shifting the partitioning of incoming solar irradiation from sensible heat to latent heat (Taha, 1997). It is also a crucial physiological activity that maintains the vitality of trees and provides evaporative cooling to help dissipate heat (Wang et al., 2011). Therefore, through transpiration, trees cool themselves and also reduce the surrounding air temperatures, with a specific study in Munich demonstrating a peak cooling effect of 3.5 °C (Rahman et al., 2017b). However, the cooling effect provided by these mechanisms is localized and varies in both space and time, with tree morphology, species characteristics, above and below-ground site conditions having considerable influence. Urban trees surrounded by impervious surfaces must tolerate harsh ecological conditions such as elevated surface and soil temperatures, limited water infiltration, inadequate nutrient availability, and impeded leaf-air gas exchange (Wang et al., 2020). This increases the trees' water stress and hampers their growth and transpiration (Gillner et al., 2017; Pretzsch et al., 2017). Such restricted growth negatively impacts the development of tree crowns, resulting in smaller canopies. A smaller canopy significantly reduces the interception of incoming short-wave radiation, consequently diminishing the tree's shading and cooling effects. Moreover, impervious surfaces not only limit water infiltration but also lead to soil compaction (McClung and Ibáñez, 2018), reducing both soil moisture and the tree roots' ability to penetrate the soil for water and

* Corresponding author
E-mail address: nayanesh.pattnaik@tum.de (N. Pattnaik).

https://doi.org/10.1016/j.jenvman.2024.121242
Received 23 January 2024; Received in revised form 10 May 2024; Accepted 24 May 2024
Available online 28 May 2024

nutrient uptake. These factors together restrict transpiration—a critical process for latent heat loss—thereby impacting the tree's capacity to cool the surrounding environment. Above all, thermal comfort, as measured using indices such as PET (Physiologically Equivalent Temperature) or UTCI (Universal Thermal Climate Index), is largely dependent on the energy fluxes of the surrounding environment (Rahman et al., 2024). Therefore, impervious surfaces absorb much more energy penetrated through the less dense canopies as well as emit higher amount of long wave radiation, worsening thermal comfort in urban areas. While the impact of impervious surfaces on tree function has been established by previous research, there remains a gap in knowledge regarding how urban trees' growth and cooling effectiveness are influenced by urbanization intensity, beyond impervious surfaces within the tree canopy. In particular, the impact of impervious surfaces on tree growth and cooling effectiveness across a range of urban environments (e.g., densely built city center vs. low density suburban areas) remains largely unexplored.

The shading benefit provided by tree canopies mainly depends on the tree's structural characteristics, such as diameter at breast height (DBH), leaf area index (LAI), tree height (Ht), crown diameter (CD), canopy volume (CV), and canopy projection area (CPA) (Rahman et al., 2020a). Additionally, underlying surfaces also affects the magnitude of shading effect. For instance, shading depth or intensity is more important when the underlying surfaces are asphalt or built surfaces, while light shading might allow for a better combination of shading effect and grass evapotranspiration when the shaded surfaces are grass lawns (Rahman et al., 2021). Similar to shading, the extent of transpiration cooling is influenced by morphological characteristics as well as physiological characteristics such as species level differences in wood anatomy, hydraulic traits and regulation of stomatal conductance in response to environmental conditions and the built environment. Winbourne et al. (2020) highlight the limited understanding of transpirations' role in urban tree cooling at local level, hindered by scarcity of data on species specific rates and variation in urban areas.

Reduction in sensible heat fluxes (through shading) and increase of latent heat flux (through transpiration) can reduce mean radiant temperature (Tmrt), hence enhance human thermal comfort (Rahman et al., 2020b). Other important variables for human thermal comfort include wind speed, humidity, and solar radiation (Lee et al., 2016). However, it is still unclear how different tree related characteristics and micrometeorological variables across different urban settings interact and affect human thermal comfort. Furthermore, previous studies have focused primarily on individual tree traits and their influence on thermal comfort, often neglecting tree growth and vitality. For instance, tree species with high LAI significantly enhance human thermal comfort by providing comfortable thermal conditions beneath their canopies (Gillner et al., 2015). However, under suboptimal growth conditions and drought-induced stress frequently observed in urban areas with high imperviousness, trees may face challenges in developing denser crowns (Rötzer et al., 2021), and might even resort to leaf shedding as an adaptive measure to tolerate heat stress (Sanusi and Livesley, 2020). Such an adaptive response, while helping trees endure harsh conditions, can also diminish the cooling benefits that were initially anticipated. Additionally, different tree species have distinct growth and physiological responses contingent to the specific urban morphology they inhabit (Rötzer et al., 2021; Shashua-Bar et al., 2010). The lack of comprehensive knowledge around the capacity of different urban tree species to deliver microclimate benefits in different urban contexts limits city planners to select right species for the right place when the aim of planting is to improve human thermal comfort.

To fill this gap, this research investigates the provisioning of the cooling effect by urban trees at different levels of urbanization. We used the gradient approach (McDonnell and Pickett, 1990) to understand the interplay and cumulative effects of tree cover and built surfaces in mitigating the urban heat in heterogenous urban landscapes. Gradient analysis examines transects extending from the urban core to the suburban or rural periphery of the city, to examine changes in ecological structure and functions as a result of urbanization (Qiu et al., 2017; Ziter et al., 2019). While the effect of urbanization on tree growth and tree cooling has been studied previously separately, the novelty in our research lies in the fact that we combine both of these aspects together. We quantify how the tree growth and vitality, cooling effectiveness and human thermal comfort provided by four commonly planted urban tree species vary along a gradient of imperviousness in Munich, Germany. Our aim is to detect the effects of imperviousness on the microclimatic regulation provided by different urban tree species. Specifically, we pose the following questions.

- How does a gradient of imperviousness affect tree growth and cooling effectiveness?
- Which species traits show the greatest influence on human thermal comfort?

2. Material and methods

The description of the study area and selection of sampled trees, along with the calculation of imperviousness density, are introduced in Sections 2.1 and 2.2. Structural and morphological measurements of the sampled trees are detailed in Section 2.3, followed by meteorological, physiological, and edaphic measurements in Section 2.4. Sections 2.5 and 2.6 outline the calculations and analyses addressing the first research question. Section 2.5 describes the tree growth analysis using tree ring data, while Section 2.6 explains the transpiration calculations used to determine latent heat loss. Section 2.7 presents the thermal comfort calculations for our second research question. Finally, Section 2.8 provides details of the statistical analysis approach.

2.1. Study area and data collection period

We conducted the study in Munich, which is the third largest city in Germany with a population of 1.59 million and a high population density (51 people/ha) (LH München, 2023). Munich has a temperate climate with warm summers and is influenced by the Alps due to its location. Munich has several large patches of green spaces distributed throughout the city (Pauleit and Duhme, 2000), with just a few structures taller than 100 m. It also has a high degree of surface sealing in the city center region (Taubenböck et al., 2021). This strongly influences the microclimate within the city, with previous studies finding that the monthly mean UHI intensity reaches up to 6 °C (Pongracz et al., 2006). The mean annual temperature was 10.1 °C and the mean annual precipitation was 939.7 mm between the period of 1991–2020 (Station: München Stadt ID:3379; DWD, 1991–2020). In 2021, when the field measurements took place, the mean annual temperature was 9.7 °C and the mean annual precipitation exceeded the long term average by 131.3 mm (DWD, 2021).

2.2. Sampling design and impervious density calculation

We identified the sites and location of four common urban tree species through an extensive field campaign. The trees were roughly selected along a continuous North-South and East-West transect, measuring approximately 8 km from the center of the city to the suburban areas in each of the four-cardinal direction, aimed to represent the impervious gradient. The final count of 38 trees from an initial inventory of 137 trees were chosen based on a number of factors. First, the selected trees were healthy and free from any visible signs of damage or decay. Additionally, there was a clear space of 1.5 times the canopy projection area around each tree to ensure they were not hindered by any obstacles or competition from surrounding trees. Secondly, logistical considerations influenced tree selection; Trees near public transport stations and with lower crown base were chosen to ease manual transport of instruments and avoid using large ladders for measurements. Along with

the logistical constraints, to eliminate any personal and instrument bias, the same instruments and personnel were used across the transect. Finally, to incorporate urban spatial heterogeneity of trees in green and gray infrastructure, parks as well as street trees were selected (See Fig. 1).

Imperviousness, measured by the imperviousness density (IMD) high-resolution layer (HRL) (EEA, 2018), was used as a proxy to identify urbanization intensity and find the percentage of impermeable surface cover. At finer scales, this metric better reflects permanent land cover change unlike other proxies such as distance to city center, population density, road density etc (McDonnell and Hahs, 2008). IMD HRL, with a 10m spatial resolution, captures level of sealing of the soil per area unit (imperviousness degree ranging from 1 to 100%) through a semi-automated classification, based on calibrated NDVI. QGIS 3.10.0-A. Coruna (https://qgis.org/en/site/) was used to do the spatial analysis for IMD determination for the study sites. To capture the background conditions in each tree's immediate vicinity, a buffer of 500m around each tree was made. This buffer range has been used in other studies to record the landscape level effects (Alonzo et al., 2021; Rahman et al., 2022). Although there might be other trees within this buffer zone which may also affect local conditions, our study design was primarily focused on individual tree and we control for potential confounding factors by conducting direct measurements on each individual tree and meteorological and edaphic variables in the vicinity.

The gradient analysis stratified tree samples into three zones based on IMD: High Imperviousness Zones (HIZ, IMD >70%), Medium Imperviousness Zones (MIZ, IMD 40–70%), and Low Imperviousness Zones (LIZ, IMD <40%). HIZ are dense and compact areas, mostly located in the inner-city district, largely commercial in nature, are characterized by greater amount of surface sealing, potentially limiting space for adequate crown and root development. MIZ represent areas that are a mix of commerce and residential areas, where there are comparatively more open spaces compared to HIZ. LIZ are characterized by low-density residential areas in suburban spaces, with considerable open spaces and providing conditions that can foster good tree growth. The distribution of tree locations, zones, and IMD values is detailed in Fig. 1 and Table 1.

2.3. Tree species selection and morphological measurements

The tree species chosen for this study are commonly planted throughout European cities (Pauleit et al., 2002), but have contrasting morphological characteristics, wood anatomy and water use strategies. *Acer platanoides* has a high shade tolerance, high photosynthetic ability and leaf area ratio (Niinemets and Valladares, 2006), and it has a diffuse to semi-diffuse porous structure (Zimmermann et al., 2021), as well seen to be isohydric although there are some contrasting studies on this. *Tilia cordata* is a shade-tolerant species with a low water use efficiency (Radoglou et al., 2009), has medium to high LAI, is diffuse porous and anisohydric (Moser-Reischl et al., 2021). *Robinia pseudoacacia* has a low LAI, is shade intolerant, very tolerant to drought, shows strong isohydric behavior and has a ring-porous wood anatomy (Moser et al., 2016). Finally, *Platanus x acerifolia* or *Platanus x hispanica* is a hybrid of *Platanus orientalis* and *Platanus occidentalis* that grows throughout Central Europe. It requires a lot of light (Roloff, 2013), is anisohydric (Rötzer et al., 2019) and has a diffuse-porous wood structure (Moser-Reischl et al., 2021).

Diameter at breast height (DBH) was measured using a diameter measurement tape at a height of 1.3 m. Tree heights were calculated using a Vertex Forestor. LAI was derived from hemispherical photographs using a Nikon camera with fisheye lens following Moser et al. (2017). Crown radii were measured in eight inter-cardinal directions (N, NE, …, NW) and crown diameter, crown projection area (CPA) as well as crown volume (CV) were calculated. Furthermore, each tree was cored to the heartwood at two directions (N-E) to estimate tree age. The structural and morphological data are detailed in Supplementary section 1.2.

2.4. Leaf physiological, micrometeorological and soil moisture measurements

We conducted measurements on 12 sunny, warm summer days spread across June, July and August. For further analysis, we selected seven out of 12 days where the maximum air temperature (AT) was greater than 27 °C and the vapor pressure deficit (VPD) was greater than

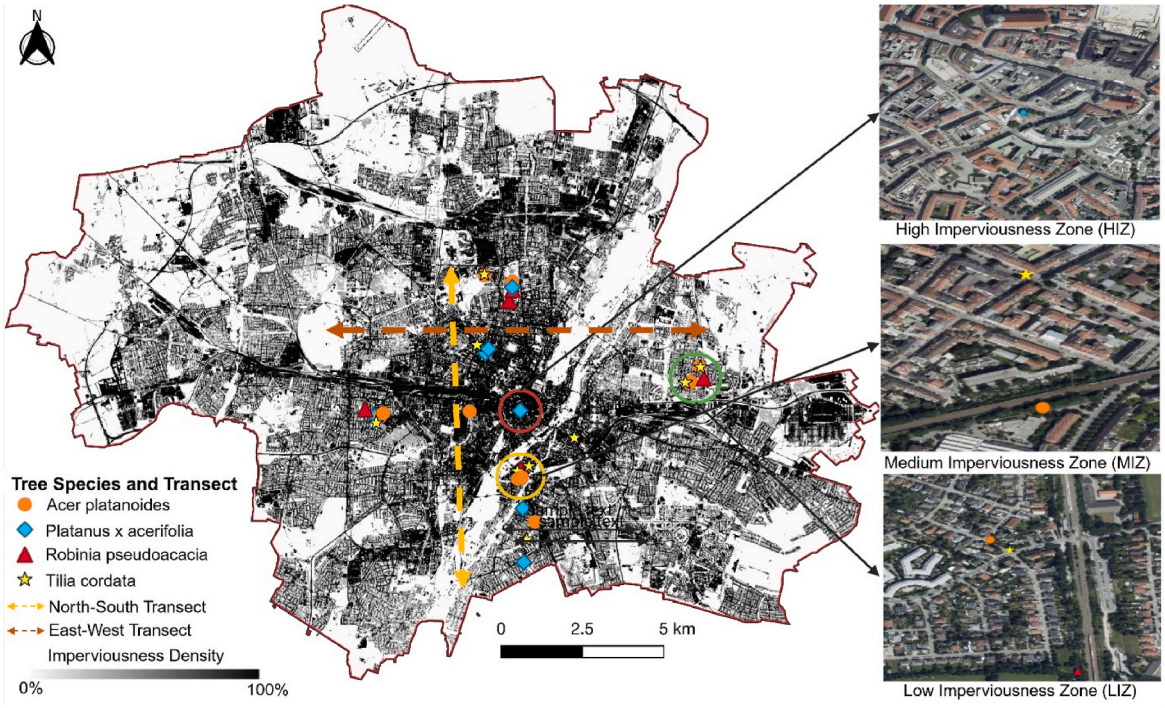

Fig. 1. Map showing location of the trees in the study, the transect followed and the imperviousness density.

Table 1
Tree species frequency and their location along different High imperviousness, medium imperviousness and low imperviousness zones in the study.

Zone	Impervious cover (%)	*A. platanoides*	*P. x acerifolia*	*R. pseudoacacia*	*T. cordata*
HIZ	>70%	3	3	2	4
MIZ	40–70%	3	4	3	2
LIZ	<40%	5	2	3	4

2.3 kPa to ensure comparability. These thresholds have been used in previous studies (Rahman et al., 2021) and also helped us to identify tree cooling performance for warmer days with high atmospheric demand, conditions that are likely to be more common in Munich in the future (Zölch et al., 2016). The meteorological conditions are detailed in Supplementary Section S1.1.

Stomatal conductance is a measure of the degree of leaf stomatal opening and is used as an indicator of plant water status (Rahman et al., 2015). Measurements of stomatal conductance were carried out on six to seven leaves (four to five sunlit leaves and two shaded leaves from the mid crown of each tree) using the leaf porometer (model SC-1, METER Group AG, Munich, Germany), and the measurements were replicated three times, resulting in 18–21 readings for each tree. These measurements, taken between 11:00 and 16:00 h, were complemented by leaf temperature readings. Simultaneously, same amount of meteorological observations of air temperature, relative humidity and wind speed were recorded concurrently at 1.5 m above the ground using a hand-held multifunction digital anemometer (PCE, model PCE-THA 10). Furthermore, the atmospheric pressure data for each measurement day were recorded from the published data of the German Meteorological Service (DWD).

Chlorophyll content, closely related to plant stress and senescence, was measured non-destructively using a chlorophyll meter (model SPAD-502Plus, Konica Minolta). The device calculates a numerical value (SPAD) which is proportional to the amount of chlorophyll present in the leaf by measuring the absorbance of the leaf in the red and near-infrared, where higher SPAD suggests a healthier plant. We measured the SPAD for the same six to seven leaves that were used for measuring stomatal conductance, resulting in 18–21 data points for each tree. Additionally, the soil moisture content was measured using a soil moisture probe. approximately 60–100 cm from the tree trunk. Surface temperatures of grass and asphalt surfaces within the canopy shade and outside the canopy were also measured using a laser gun (PTD 1, Bosch GmbH, Germany). The shaded measurement was always close to the tree trunk, while outside the canopy measurements were always a minimum of 5 m away from the shade. The surface temperature reductions (ΔST) was calculated from the difference of sunny and shady surface temperature.

Midday leaf water potential, indicative of tree water use and water stress, was measured using a Scholander bomb on 14 selected tress from the sample representing the four species. These measurements were conducted in July and August between 11:00 h to 15:00 h, on two sunlit and one shaded leaf from each tree's mid-crown.

2.5. Tree growth analysis

Differences in tree growth and vitality between the species significantly affect the magnitude of ecosystem services provided by the trees (Pretzsch et al., 2017; Rötzer et al., 2019). The annual growth patterns of urban trees can indicate their growth conditions and provide insights into the response of trees to external factors. Using dendrochronology in this context, two cores per tree were extracted at breast height (1.3 m) to analyze the basal area over a long timeseries. The tree ring width, specific age and basal area were determined following (Dervishi et al., 2022; Franceschi et al., 2023; Honold, 2021; Moser et al., 2016). The tree ring analysis for carried out for period of 50 years from 1970 to 2020. Basal area (BA) and basal area increment (BAI) were calculated using annual radial growth of the increment cores through a stepwise back-calculation starting from the year 2020.

2.6. Transpiration and energy loss calculation

The transpiration rates (E, mmol m^{-2} s^{-1}) of the leaves were calculated from the stomatal conductance and meteorological data following (Rahman et al., 2011):

$$E = g * (e_{leaf} - e_a) / P_a \quad (1)$$

Where, g is the total conductance of water vapor (mmol m^{-2} s^{-1}), e_{leaf} is the vapor pressure inside the leaf, which was assumed to be saturation vapor pressure at leaf temperature, e_a is the vapor pressure of the atmosphere, which is calculated by multiplying vapor pressure at air temperature by the relative humidity of the air and P_a is the atmospheric pressure (kPa). Saturation vapor pressure at leaf temperature (e_{leaf}) is given by Tetens formula:

$$e_{leaf} = 0.611 * e^{\frac{17.6*T_l}{T_l+240.97}} \quad (2)$$

$$e_a = e_{leaf} * T_a * RH \quad (3)$$

where, T_l is the leaf temperature, T_a is the air temperature in °C and RH is the relative humidity. The energy loss per unit leaf area (Wm^{-2}) expressed as the latent heat flux is obtained by multiplying the transpiration rates (converted to $gm^{-2}s^{-1}$) from Eq. (1) with the latent heat of vaporization ($2.45kJg^{-1}$).

Sensible heat fluxes (Q_H) were calculated using the measured surface temperature, air temperature and wind speed. Q_H was calculated for the following surfaces - shaded grass, shaded impervious, sunny grass and sunny impervious for each tree. Q_H calculation is provided in Supplementary (Section S2).

2.7. Human thermal comfort – PET calculations

PET, a commonly used human thermal comfort index (Höppe, 1999) was calculated with the RayMan Model (RayMan Pro version 1.2) (Matzarakis et al., 2010) software. As a micro-scale model, RayMan computes radiation fluxes, which are important biometeorological input for PET. For this study, specific input parameters were: date and time of the collection data, location, tree geographical data (longitude, latitude, altitude), meteorological conditions such as air temperature (°C), relative humidity (%), wind speed (m/s). Personal data in terms of height (m), weight (kg), age, sex, clothing, and activity were kept default.

2.8. Statistical analysis

Statistical analyses were performed in R version 4.2.3. Structural variables from the trees (DBH, Tree height, Age, CPA, LAI, Crown start) were subjected to two-way Analysis of variance (ANOVA) and Tukey post hoc tests to see significant difference ($p < 0.05$) between the species and the imperviousness zones.

Linear mixed models (LMM) were developed to assess the influence of imperviousness (HIZ/MIZ/LIZ; *Zone*) on different growth and physiological variables. Mixed models from "lmer4" package with Kenward-Roger approximation of F-statistics, and post hoc comparisons using the "emmeans" package were used. These models can also quantify the effect of imperviousness on PET. Models for annual basal area (*BA*) derived from tree cores, micrometeorological data (Surface temperature

reduction (*ST*), sensible heat flux (*Qh*)) and different tree physiological traits such as stomatal conductance (*SC*), Energy loss (*Eloss*), SPAD, were performed separately. If the dependent variable satisfied the condition of normal distribution (examined by the Shapiro-Wilk test), then they were modeled using a linear mixed model using lmer function. If not, they were modeled using a generalized linear mixed model (GLMM) using glmer function.

The fixed effects were chosen accordingly to our research questions. In the LMMs for *BA* for each of the species, main effects included the location (HIZ, MIZ, LIZ) and *age*. In the LMMs for other variables, main effects were the location (HIZ, MIZ, LIZ) and species (*A. platanoides, R. pseudoacacia, P. x acerifolia, T. cordata*). Random effects included tree identity (Tree ID) and date (Date), to account for the repeated measures and differences between the individual trees that could affect the outcome due to spatial and temporal dependencies. P- values were examined to see the significance of the effects. The final models are shown below:

$$lmer\ (\ln(BA) \sim \ln(Age) \times Zone + (1|Tree\ ID)) \quad (2)$$

$$lmer\ (\text{SPAD} \sim\ \text{Species} \times Zone + (1|Date) + (1|Tree\ ID)) \quad (3)$$

$$glmer\ (\text{SC}\ /\ \text{Eloss}\ /\ \text{ST}\ /\ \text{Qh} \sim\ \text{Species} \times Zone + (1|Date) + (1|Tree\ ID)) \quad (4)$$

For the second research question, an information–theoretic framework was employed to determine the relative importance of significant explanatory variables on PET, and multimodel inference (Grueber et al., 2011) was used to estimate the parameters. Supplementary Table 4 shows all the variables that were considered. A stepwise procedure was followed to select the relevant variables for further analysis. First, we generated scatter plots to visualize linear relationships between the PET and the predictor variables, followed by computing Pearson correlation coefficients to check for correlation. Furthermore, collinearity among the predictor variables was assessed through the use of VIF (Variance Inflation factor). Highly correlated variables (>0.7) were excluded (Zuur et al., 2010). Five variables out of the initial eleven variables were retained through this process. We standardized variables using z-scores for comparability. A GLMM using glmer function fitted to a gamma distribution with log-link function was created, which is suitable for modeling variables that show a skewness in their distribution, such as PET in our case. We then generated an initial set of candidate models (n = 32 for the five predictor variables) for all possible combinations of the considered predictor variables using the 'dredge' function. From the generated candidate models, we selected the best approximating models based on the smallest difference in Akaike Information Criterion (AICc). Models within 10 AICc units of the most parsimonious were retained for inference (Burnham et al., 2002). The relative importance of predictors in the GLMM was assessed by summing Akaike weights, yielding model-weighted average parameter estimates, incorporating model selection uncertainty (Burnham et al., 2002).

3. Results

3.1. Tree growth and vitality across the zones of imperviousness

3.1.1. Tree annual radius and basal area growth

Tree ring analyses yielded growth curves for the sampled tree species across the gradient from 1970 to 2020 (Supplementary Fig. 1). In general, annual radius increment of trees located in LIZ (mean growth = 3.94 mm/year) were highest followed by trees located in MIZ (mean growth = 3.76 mm/year) and HIZ (mean growth = 3.32 mm/year). Overall, we observe higher BA values over age for all the species in LIZ, except for *R. pseudoacacia* (Fig. 2). Minimal relative differences in size among the different species are observed during the younger ages. However, distinct growth patterns are observed after the trees reach the age of 25. In particular, *P. x acerifolia* exhibited a significantly faster

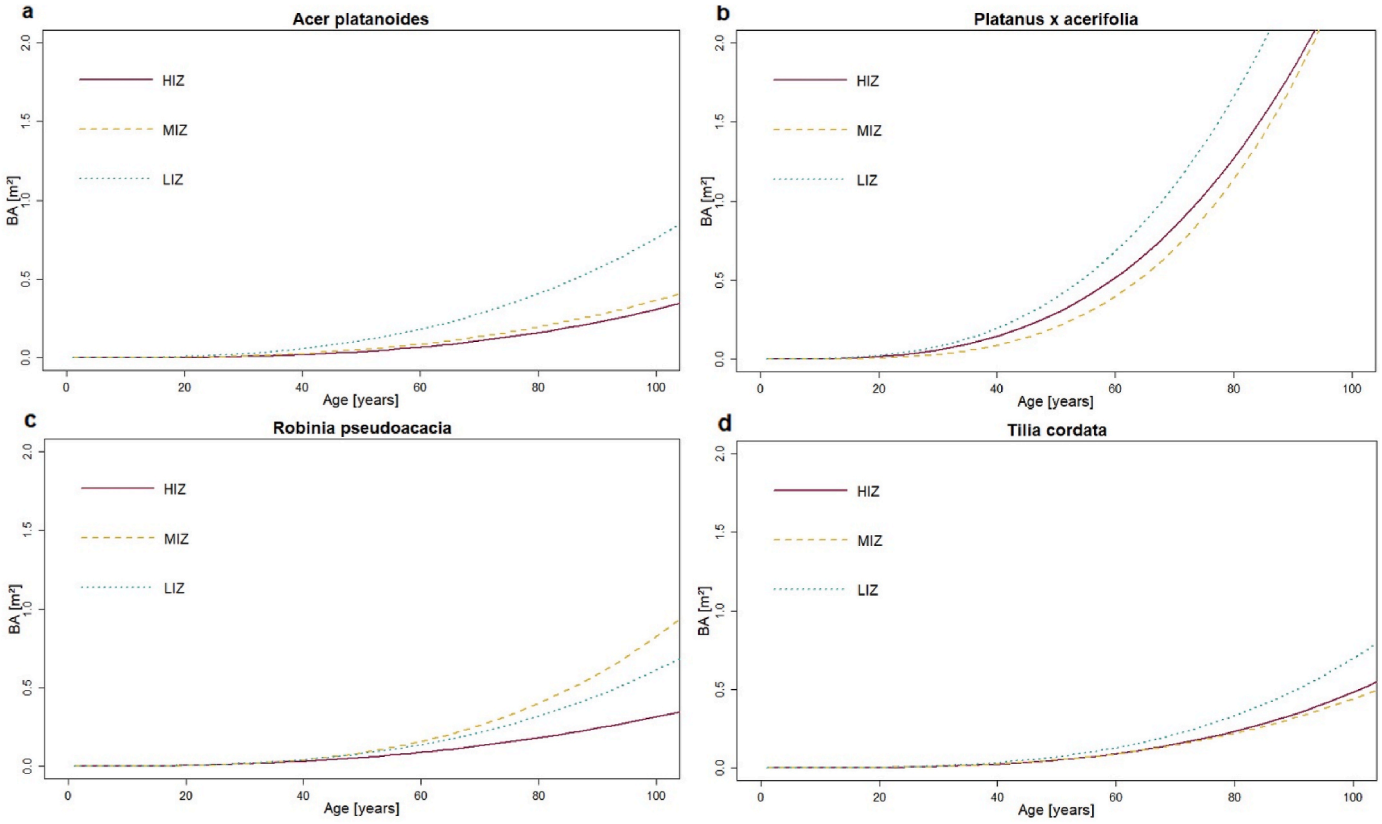

Fig. 2. Logarithmic relationship between Basal Area and Age of the studied species across the zones of imperviousness.

growth rate compared to the other three species studied in all the zones of imperviousness. While growing in LIZ and at the age of 60, *P. x acerifolia* exhibit approximately 40% higher BA compared to those in the MIZ, and about 25% higher BA compared to those in the HIZ. In contrast, for *T. cordata* trees of similar age, those in the LIZ display a 30% higher BA compared to both the HIZ and MIZ. Notably, *A. platanoides* trees present the most significant variation. A 60-year-old *A. platanoides* in the LIZ has a 58% and 47% larger BA compared to counterparts in the HIZ and MIZ, respectively.

3.1.2. Chlorophyll content and leaf water potential

SPAD value showed significant differences both among tree species and impervious zones (Fig. 3). The mixed model results revealed a significant difference in SPAD among impervious zones ($F(2,78) = 3.16$, $p < 0.05$) and across different tree species ($F(3,78) = 10.54$, $p < 0.0001$). The HIZ generally had the lowest SPAD values for all species (Fig. 4). Among species, *T. cordata* showed the highest SPAD values (Mean SPAD value = 39.6), followed by *A. platanoides* (Mean SPAD value = 34.5), *R. pseudoacacia* (Mean SPAD value = 32.7) and *P. x acerifolia* (Mean SPAD value = 32). *P. x acerifolia* trees in the LIZ demonstrated an approximate 8% higher SPAD value compared to those in the MIZ, and a 20% higher value compared to those in the HIZ. Similarly, the *A. platanoides* trees in the LIZ exhibited 9% and 11% higher SPAD values compared to those in the MIZ and HIZ, respectively. However, *T. cordata* and *R. pseudoacacia* displayed their highest SPAD values in the MIZ, rather than the LIZ. Specifically, *T. cordata* in the MIZ displayed 7% and 4% higher SPAD values compared to those in the HIZ and LIZ, respectively. Similarly, *R. pseudoacacia* in the MIZ showed 21% and 6% higher SPAD values compared to those in the HIZ and LIZ.

Significant differences were observed in the leaf water potential of the studied species (Table 2). *T. cordata* had the lowest (most negative) leaf water potential (-3.12 ± 0.29), followed by *P. x acerifolia* (-2.74 ± 0.21), *A. platanoides* (-2.31 ± 0.13) and *R. pseudoacacia* (-1.88 ± 0.36).

3.2. Tree cooling potential across the impervious zones

3.2.1. Surface cooling

Tree species differed significantly in terms of surface temperature reductions (ΔST) over impervious surfaces ($F(3,78) = 5.1$, $p < 0.01$); however, not between the zones. In case of ΔST over grass surfaces, we found no significant differences between species or zones. ΔST over impervious surfaces was significantly higher than over grass surfaces (Fig. 4). On average ΔST over impervious surfaces was 15.5 °C, while ΔST over grass surfaces was 6.8 °C. *T. cordata* (Mean = 22.0 °C) had the highest ΔST over impervious surfaces, followed by *A. platanoides* (Mean = 18.05 °C), *P. x acerifolia* (Mean = 16.1 °C) and then *R. pseudoacacia* (Mean = 14.6 °C). ΔST over grass surfaces was highest with *R. pseudoacacia* (Mean = 8.94 °C), followed by *A. platanoides* (Mean = 8.5 °C), *P. x acerifolia* (Mean = 8.0 °C) and *T. cordata* (Mean = 7.8 °C). Furthermore, ΔST was strongly correlated to LAI (Supplementary Fig. 2). The correlation between ΔST over impervious surfaces and LAI was higher ($r = 0.51$, $p < 0.001$) than the ΔST over grass surfaces and LAI ($r = 0.27$, $p < 0.05$).

3.2.2. Surface energy fluxes over different species and surfaces

Both shaded grass and impervious surfaces showed lower surface temperature compared to the air temperature as shown by the negative sensible heat fluxes and opposite for the sunny surfaces. There were no significant differences found over different zones or between the species. Change in sensible heat fluxes (ΔQ_h) from sun-exposed to shaded condition was larger in impervious surfaces compared to grass surfaces (Fig. 5).

3.2.3. Stomatal conductance and transpirational cooling

Stomatal conductance differed significantly among impervious zones ($F(2,78) = 5.76$, $p < 0.01$) and across different tree species ($F(3,78) = 24.25$, $p < 0.0001$). Non-significant interaction was found between species and impervious zone. In general, trees in LIZ had the highest rate of stomatal conductance, followed by MIZ and then HIZ (Supplementary Fig. 3). *P. x acerifolia* (288 mmol/m^2/s) showed the highest mean stomatal conductance across the transect, followed by *T. cordata* (199 mmol/m^2/s), *R. pseudoacacia* (170 mmol/m^2/s) and *A. platanoides* (168 mmol/m^2/s). Post-hoc analysis showed that the stomatal conductance for *T. cordata*, *A. platanoides* and *R. pseudoacacia* were found to be highest in the LIZ, whereas *P. x acerifolia* in the MIZ.

Transpirational cooling, assessed through energy loss per unit leaf area, revealed significant differences among species ($F(3,78) = 13.96$, $p < 0.001$) and across the impervious zones ($F(2,78) = 3.70$, $p < 0.05$) (Fig. 6). However, the interaction between species and zone exhibited no significant effect. The highest rate of energy dissipation occurred in the LIZ, followed by the MIZ, and then HIZ. *P. x acerifolia* consistently

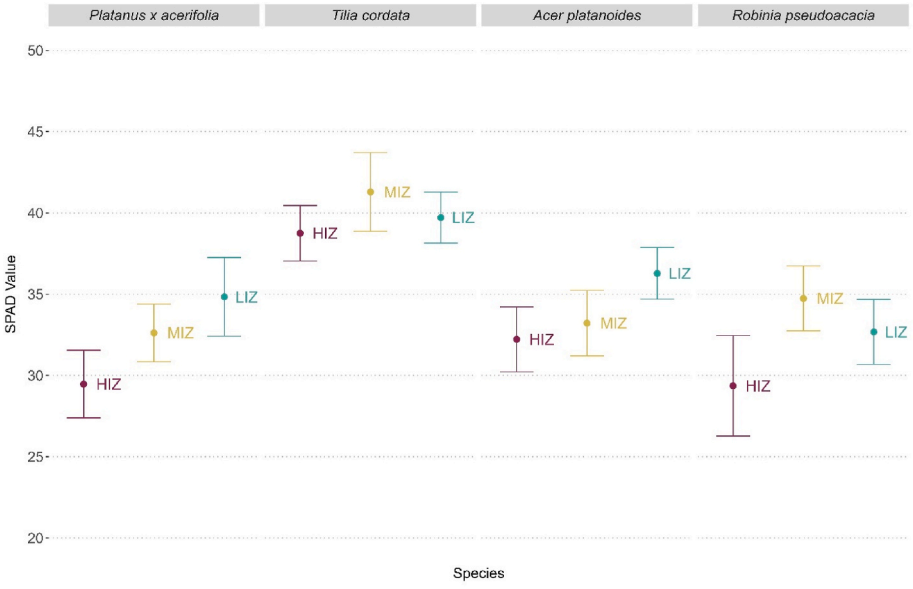

Fig. 3. SPAD values for different tree species across the zones of imperviousness. The dot indicates the mean value, and the whiskers indicate the corresponding standard error.

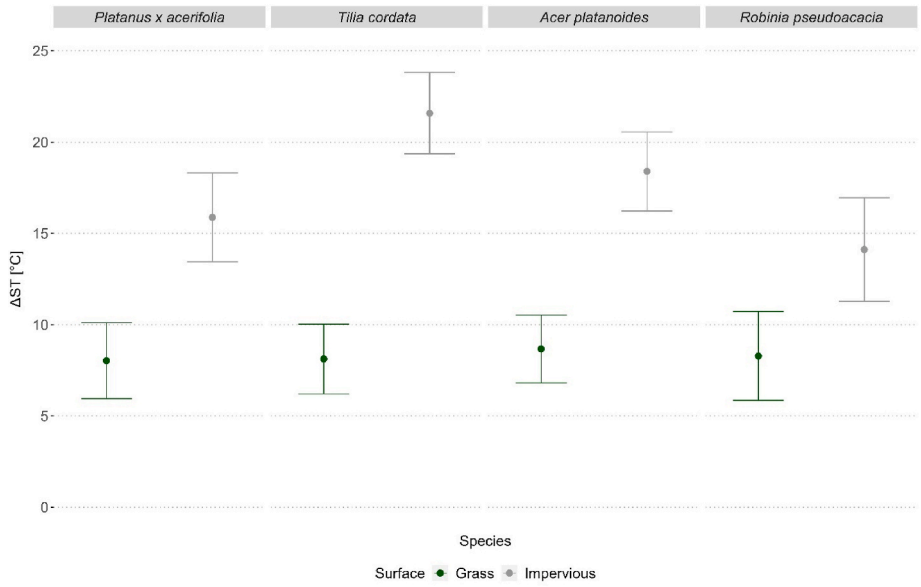

Fig. 4. Surface temperature reductions (ΔST) potentials of the different tree species across the zones of imperviousness. The dot indicates the mean value, and the whiskers indicate the standard error.

Table 2
Midday Leaf Water Potential of the studied tree species (Mean ± SE).

Tree species	Leaf Water Potential (MPa)
Platanus x acerifolia	−2.74 ± 0.21
Tilia cordata	−3.12 ± 0.29
Acer platanoides	−2.31 ± 0.13
Robinia pseudoacacia	−1.88 ± 0.36

showed the highest transpirational cooling, with a mean value of 317 W m^{-2} followed by *T. cordata* at 221 W m^{-2}, *R. pseudoacacia* at 196 W m^{-2}, and *A. platanoides* at 188 W m^{-2}. Moreover, both *P. x acerifolia* and *T. cordata* displayed a comparable 11% increase in their transpirational cooling from the lowest observed values in HIZ and MIZ respectively to LIZ. Meanwhile, *A. platanoides* demonstrated the most pronounced variation, with an almost 47% increase in transpirational cooling when transitioning from HIZ to LIZ. Similarly, for *R. pseudoacacia*, this increase was substantial, at 36% over the same gradient.

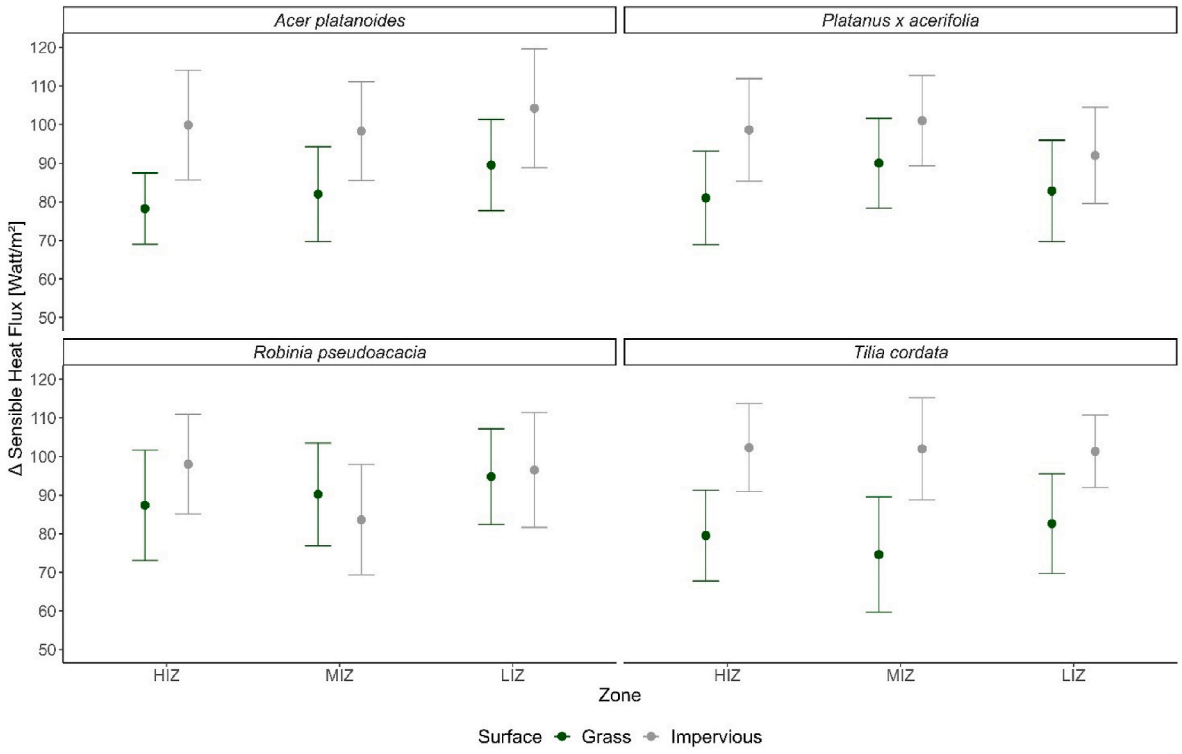

Fig. 5. Delta Sensible Heat Fluxes values (Sun-Shade) over grass and impervious surfaces calculated for the different tree species across the zones of imperviousness. The dot indicates the mean values, and the whiskers indicate the standard error. (For interpretation of the references to colour in this figure legend, the reader is referred to the Web version of this article.)

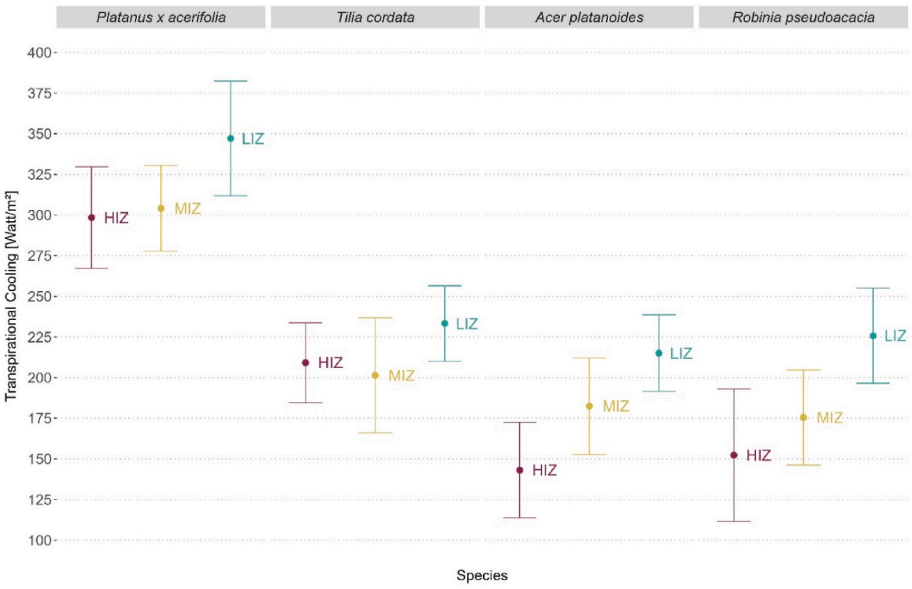

Fig. 6. Transpirational cooling vis energy loss of the different tree species across the different zones of imperviousness. The dot indicates the mean value, and the whiskers indicate the corresponding standard error.

3.3. Relative importance of Tree traits on PET

The reduced GLMM model consisted of LAI, CPA, Sealing, SC, and Tree height (Ht) as significant fixed effects. Of the 32 models that were considered, only 13 models met the criteria for a good fit with $\Delta < 10$. These 13 models were then used to estimate the average values of the predictor variables. The model that provided the best approximation included all of the significant variables. The marginal R^2 was 0.48, indicating that the fixed effects accounted for a significant proportion of the variance in the model. However, with the inclusion of random effects, the conditional R^2 was 0.73. Based on the Akaike sum of weights, among all the variables, LAI was found to have the highest weight (0.993). The second most important variable was CPA with a weight of 0.876. The remaining three variables, Sealing, Ht, and SC, showed a smaller difference in their weights, with Sealing having the third-highest weight of 0.782, followed by Ht with a weight of 0.761, and finally SC with a weight of 0.752.

4. Discussion

Our findings indicate that trees provide better surface cooling in HIZ compared to MIZ or LIZ, mainly because of the higher proportion of impervious surfaces. However, trees in areas characterized by low impervious cover (LIZ in our case) grow better and also exhibit the highest potential for transpirational cooling. While prior research involving remote sensing reported higher land surface temperatures in areas with higher imperviousness (Wang et al., 2022), our study, which involves ground-based tree-level measurements, offers a more micro-scale perspective. Our results align closer to the findings of Rahman et al. (2022), who used ground-based meteorological stations across an urban-suburban transect and reported better cooling efficiencies of urban greenspaces at sub-urban areas.

Furthermore, our study revealed significant species-specific variations in physiological and growth responses. Fastest-growing species in our study, *P. x acerifolia*, exhibited the highest potential for cooling. This was evident from both the transpirational cooling and the substantial reductions in surface temperature, even though it did not possess the highest LAI or the highest chlorophyll content. These findings bear resemblance to those of Rahman et al. (2015), who compared five commonly planted urban tree species in Manchester, UK., and demonstrated that fast-growing species with higher growth rate and high stomatal conductance contribute to high cooling potential, albeit with the trade-off of higher water stress.

4.1. Effect of imperviousness on growth of urban trees

In our study, trees of the same age growing in LIZ have larger basal area on average than the trees in HIZ and MIZ. Our findings are consistent with some literature that has used dendrochronology to examine the impact of urbanization on tree growth, but contrasting results have also been reported. For instance, Schneider et al. (2022) found faster growth rate in urban trees than their rural counterparts across an inner-city to rural transect in Berlin, while Dahlhausen et al. (2018) observed that *T. cordata* trees grew at a faster rate in densely built-up areas. However, studies by Pretzsch et al. (2017) and McClung and Ibáñez (2018) did not find significant growth differences between urban and suburban trees, with the latter finding that increasing impervious cover reduced the growth of *Acer saccharum* and *Quercus rubra* across an urbanization gradient in Michigan, US. Franceschi et al. (2023) corroborated our findings, reporting significantly higher basal area increment values for *A. platanoides and T. cordata, while P. x acerifolia* and *R. pseudoacacia* showed small but insignificant differences, in suburban settings as opposed to urban surroundings in Munich.

Growth rates are also highly species specific, with different trees showing different responses towards light, temperature, nutrients and water (Moser-Reischl et al., 2021). Although high imperviousness affected the growth of each of the species, in our present study, *R. pseudoacacia* was the only tree species which seem to cope comparatively better in high imperviousness zone. This is in line with the results found by Moser et al. (2018) with better growth rates for *R. pseudoacacia* close to city center as compared to city periphery. Similar to Moser--Reischl et al. (2021), the present study also confirms *P. x acerifolia* as a fast-growing species as it showed the highest growth rate across all the species.

The comparatively lower growth rates observed in the HIZ could be attributed to the lower soil moisture content measured (Supplementary Table 2). Inadequate access to essential water resources, combined with restricted root volumes and suboptimal substrate quality, can hamper tree growth (Rötzer et al., 2021). In the face of future elevated urban temperatures and drought, such local growing conditions might get worse for trees. While our analysis sheds light on the observed growth differences between species and impervious zones, it is essential to

acknowledge the inherent limitations in our study. Gradient analysis, by nature, lack ceteris paribus conditions, potentially leading to confounding factors influencing the diverse growth responses. Factors beyond imperviousness, such as pollution and ground water levels (Moser et al., 2018), anthropogenic influences, which can vary significantly between city center and suburban areas, can also affect the tree growth and vitality. Therefore, future research should incorporate broader array of environmental variables and different anthropogenic influences, to further understand complex interplay of urban conditions on tree vitality.

4.2. Effect of imperviousness on cooling potentiality of urban trees

Our study reveals that a 10% increase in imperviousness underneath tree crown corresponds to a PET rise of 0.11 °C, although marginal, highlight the relationship between impervious surfaces and localized urban thermal conditions. Trees with dense canopies were found to play a significant role in surface cooling, consistent with the existing literature. Across different impervious zones, the surface cooling remained consistent, with an average reduction in surface temperature of 15.5 °C over impervious surfaces, exceeding the 12 °C documented by Armson et al. (2012) in their Manchester study. This difference may be attributed to differences in tree age, size and the atmospheric condition in a Central European city compared to Manchester, UK. The trees examined in Manchester were comparatively younger and smaller, potentially casting a lighter shade compared to the mature, well-developed crown trees in our study. Furthermore, our research underscores that the cooling potential offered by tree shade is also contingent on the nature of the surface beneath the trees. Sensible heat flux of impervious surfaces beneath depended heavily on the LAI, as the sensible heat flux of *T. cordata* was more negative followed by *A. platanoides*, *P. x acerifolia* and *R. pseudoacacia*. This aligns with the conclusions drawn in prior studies (Massetti et al., 2019; Rahman et al., 2020b).

The significant differences in leaf-level physiology at different zones and tree species within our study have a direct impact on tree-water relations, ultimately influencing the latent cooling capacity provided by trees. In contrast to our findings, Lahr et al. (2018) reported higher rates of stomatal conductance for *Acer rubrum* trees along urban areas compared to those in suburban areas. This discrepancy may be attributed to the differences in Vapor Pressure Deficit during their measurements (1–2 kPa), as opposed to our study where VPD exceeded 2.3 kPa. Previous research has established VPD as a significant driver of leaf gas interactions, potentially explaining this variance. Our results align more closely with Rahman et al. (2017a) who investigated the transpirational cooling of *T. cordata* trees and observed significantly higher water loss in a less impervious site compared to a more impervious one in Munich.

Stomatal conductance and transpiration values measured in our study for all the tree species were slightly higher than previously reported in literature (Jiao et al., 2016; Konarska et al., 2016; Moss et al., 2019; Rötzer et al., 2019). This could possibly be explained by our measurement period as we selected warm, sunny hours to conduct our measurements when the evaporative demand of the atmosphere was high. Therefore, the values are rather snapshots of the higher possible values rather the diurnal average. Additionally, it is important to consider the methodological differences in transpiration measurements. Our approach utilized a porometer to gauge leaf-level transpiration, a method that may lead to overestimation compared to canopy-level transpiration assessments conducted using sap flow sensors (Rahman et al., 2017a). Across different zones, all tree species exhibited a consistent trend of displaying lower stomatal conductance in the High Imperviousness Zone and the highest values in the Low Imperviousness Zone. Despite selecting contrasting species, the differences in their physiological responses were less pronounced than expected. This could be attributed to our study design and the nature of the transect, where we measured under specific conditions to ensure comparability, leading to a limited number of samples for some species in certain zones. Future studies which can incorporate larger samples for each species could possibly tease out such differences. However, we also found our results contrasting with previous studies, particularly in the case of *R. pseudoacacia* (Jiao et al., 2016; Moser-Reischl et al., 2021), possibly due to the methodological differences highlighted previously. *R. pseudoacacia* is a ring-porous, isohydric species which maintains stable mid-day leaf water potential, primarily through the mechanism of stomatal closure. Conversely, *P. x acerifolia*, *T. cordata*, and *A. platanoides*, categorized as anisohydric species, maintain open stomata without discernible thresholds in mid-day leaf water potential, rendering them more susceptible to hydraulic failure. Nevertheless, these anisohydric trees seem capable of meeting their water requirements and provide transpirational cooling in highly impervious environments by developing deep and wide rooting systems even under unfavorable urban soil and conditions (Rahman et al., 2020b; Rötzer et al., 2019). However, a closer investigation with measurements from leaf water potentials provide us a deeper understanding (Table 2). Interestingly, *P. x acerifolia* and *T. cordata*, transpired at the expense of lower (more negative) leaf water potential in High imperviousness zones, while *R. pseudoacacia* stayed true to its isohydric nature and maintained its leaf water potential across the gradient. Actively transpiring under low soil moisture conditions might increase the latent heat flux and cool down the surrounding environment, but this also makes these trees vulnerable to physiological stress and hydraulic failure. This is especially true for highly urbanized settings, where water availability is a big limiting factor, which was also observed in our measurements in the HIZ.

4.3. Tree traits for optimal human thermal comfort

The estimates from LMM for LAI, SC, and CPA were negative, indicating that these variables had a negative correlation with PET. Conversely, the Ht and Sealing had a positive effect size, suggesting that an increase in height and the amount of sealed surface within the tree canopy led to an increase in PET. Tmrt i.e., the exchange of radiant fluxes between a human and their surrounding environment, is important for human thermal comfort, more so than air temperature alone (Thorsson et al., 2007). Therefore, the reduction of sensible heat fluxes under the tree shade and the underlying surfaces are more important. Dense canopies providing deeper shade, thus showed robust correlation in the present study similar to the findings of the recent meta-analysis by Rahman et al. (2020a). *T. cordata* trees with the highest LAI, had ΔST of ca. 8 °C more than compared to *Robinia* trees, which had the lowest LAI.

Following LAI, CPA emerged as the next most influencing variable on PET in our study. This aligns with previous research highlighting the importance of canopy size such as (Ren et al., 2022) who observed that PET of streets with high canopy cover were, on average, 13.7 °C cooler than streets with low canopy cover. Wider-crowned trees reflect a greater portion of solar irradiation and cast shade over a larger area, minimizing energy absorption on underlying surfaces and diminishing re-emission of sensible heat, thereby mitigating local heat stress (Rahman et al., 2017a).

The percentage of sealing emerged as the subsequent influential factor, underscoring the importance of the underlying surface beneath the tree canopy. Controlled experiments by Shashua-Bar et al. (2011) demonstrated the combined effects of trees and well-watered grass on human thermal comfort in dry climates. This finding is corroborated by. Similarly, empirical study by Rahman et al. (2020a), found better thermal comfort provided by *R. pseudoacacia* trees in the presence of adequately moistened grass within the crown. Our study also observed a reduction in sensible heat flux and increase of latent heat flux under the grass surfaces of *R. pseudoacacia* trees, likely attributable to the tree's enhanced water use efficiency and increase amount of radiation through the light dense canopies. This prompts further investigation into the synergistic effects of various other forms of UGI, like grass and shrubs, prevalent in urban environments, to optimize human thermal comfort.

Future studies are warranted to quantify these effects and explore potential synergies or trade-offs in terms of human thermal comfort.

Contrary to established research, we found that taller trees slightly increase the PET at pedestrian level. Taller trees provide extensive shade over urban surfaces, reducing the air heating nearby. However, previous research such as that of Wang et al. (2023), propose the existence of a threshold beyond which tree height might cease to contribute significantly to near-surface cooling. Moreover, their study hinted at a potential time-dependent nature of this relationship. Considering the discrepancies between our findings and established literature, it's plausible that our measurements, conducted during hours closer to solar noon (13:30 h in Munich) when the area under the tree shadow can be less, might have influenced the observed impact of tree height on PET.

Stomatal conductance and transpiration had a relatively lower influence compared to other tree traits on human thermal comfort in our study. Previous studies have shown that tree cover reduces the temperatures of urban environments at neighborhood scales primarily through transpiration, leading to boundary layer cooling (Smithers et al., 2018). However, at a pedestrian scale, transpirational cooling is most perceptible during low wind speeds (Manickathan et al., 2018), possibly because higher wind speeds and strong advection nullifies the temperature differences within and outside the canopy. Thus, shading, influenced by canopy cover and density, emerges as a more influential cooling mechanism at pedestrian scale. Despite this, transpiration-induced cooling plays a crucial role in reducing intra-urban temperature, particularly in conditions of high atmospheric demand (Konarska et al., 2016; Lindén et al., 2016). Nevertheless, this comes with a caveat. Trees transpiring despite water stress in urban environments may provide cooling, but they also face the risk of physiological stress, as evidenced in our case with *P. x acerifolia* and *T. cordata* compared to *R. pseudoacacia*. Therefore, the strategic selection of drought tolerant species, combined with a high LAI and adequate soil moisture, can provide robust cooling through shading and transpiration. In summary, based on our analysis of investigated traits, we rank the following traits to relative significance to PET: LAI > CPA > Sealing% > Height > Transpiration.

5. Conclusion

In this study, the proportion of impervious surfaces at a local scale influenced tree growth, vitality, and physiological functions, possibly due to low soil moisture content, which in turn affects the cooling benefits provided by trees. The study quantified the adverse effect of urban imperviousness on human thermal comfort underneath tree crowns, evident in the analysis wherein a 10% increase in impervious surfaces correlates with a 0.1 °C rise in PET. While several tree traits exhibit significant effects on cooling potential, our findings highlight the paramount importance of LAI, also emphasizing that shade benefit is more effective than transpiration cooling at the pedestrian level in particular at the highly impervious city centers. Our results have several important implications in the management of urban environments to optimize human thermal comfort. Selecting suitable tree species, considering their growth and ecosystem service provisions, becomes crucial for thermal comfort optimization. Whereas transpiration plays a vital role in boundary layer cooling, species with higher stomatal conductivity and anisohydric characteristics such as *P. x acerifolia* might be important for UHI mitigation at the city scale, particularly effective in low impervious sub-urban zones. Thus, species-specific strategic planning along different levels of urbanization is important for future tree planting in relation to heat mitigation and human thermal comfort. Future research endeavors should try to establish the differences in species in different planting scenarios in different impervious zones. This will significantly contribute to the science of optimal species selection, further refining our understanding and enhancing sustainable urban environments.

CRediT authorship contribution statement

Nayanesh Pattnaik: Writing – review & editing, Writing – original draft, Visualization, Methodology, Formal analysis, Data curation. **Martin Honold:** Writing – review & editing, Methodology, Investigation, Data curation. **Eleonora Franceschi:** Writing – review & editing, Methodology, Investigation, Data curation. **Astrid Moser-Reischl:** Writing – review & editing, Visualization, Methodology. **Thomas Rötzer:** Writing – review & editing, Funding acquisition. **Hans Pretzsch:** Writing – review & editing, Investigation, Funding acquisition. **Stephan Pauleit:** Writing – review & editing, Supervision, Resources, Funding acquisition. **Mohammad A. Rahman:** Writing – review & editing, Supervision, Project administration, Methodology, Conceptualization.

Declaration of competing interest

The authors declare that they have no known competing financial interests or personal relationships that could have appeared to influence the work reported in this paper.

Data availability

Data will be made available on request.

Acknowledgments

We thank the Deutsche Forschungsgemeinschaft (DFG) for funding the project "Impact of trees on the urban microclimate under climate change: Mechanisms and ecosystem services of urban tree species in temperate, Mediterranean and arid major cities" (grant number PR 292/21–1 and PA 2626/3–1). We also thank Ms. Alejandra Zelada, Mr. Amjad Hijazin and Mr. Alaa Amer for their help in the field work. We thank the municipality of Munich for the permission to measure the trees and extract tree cores.

Appendix A. Supplementary data

Supplementary data to this article can be found online at https://doi.org/10.1016/j.jenvman.2024.121242.

References

Alonzo, M., Baker, M.E., Gao, Y., Shandas, V., 2021. Spatial configuration and time of day impact the magnitude of urban tree canopy cooling. Environ. Res. Lett. 16 (8), 084028 https://doi.org/10.1088/1748-9326/ac12f2.

Armson, D., Stringer, P., Ennos, A.R., 2012. The effect of tree shade and grass on surface and globe temperatures in an urban area. Urban For. Urban Green. 11 (3), 245–255. https://doi.org/10.1016/j.ufug.2012.05.002.

Burnham, K.P., Anderson, D.R., Burnham, K.P., 2002. Model Selection and Multimodel Inference: A Practical Information-Theoretic Approach, second ed. Springer.

Buyantuyev, A., Wu, J., 2010. Urban heat islands and landscape heterogeneity: Linking spatiotemporal variations in surface temperatures to land-cover and socioeconomic patterns. Landsc. Ecol. 25 (1), 17–33. https://doi.org/10.1007/s10980-009-9402-4.

Dahlhausen, J., Rötzer, T., Biber, P., Uhl, E., Pretzsch, H., 2018. Urban climate modifies tree growth in Berlin. Int. J. Biometeorol. 62 (5), 795–808. https://doi.org/10.1007/s00484-017-1481-3.

Dervishi, V., Poschenrieder, W., Rötzer, T., Moser-Reischl, A., Pretzsch, H., 2022. Effects of climate and drought on stem diameter growth of urban tree species. Forests 13 (5), 641. https://doi.org/10.3390/f13050641.

DWD, 2021. Deutscher Wetterdienst. www.dwd.de.

EEA, 2018. Copernicus land Monitoring service – high resolution layer imperviousness: product specifications document. https://land.copernicus.eu/en/products/high-resolution-layer-imperviousness.

Endreny, T., Santagata, R., Perna, A., Stefano, C.D., Rallo, R.F., Ulgiati, S., 2017. Implementing and managing urban forests: a much needed conservation strategy to increase ecosystem services and urban wellbeing. Ecol. Model. 360, 328–335. https://doi.org/10.1016/j.ecolmodel.2017.07.016.

Franceschi, E., Moser-Reischl, A., Honold, M., Rahman, M.A., Pretzsch, H., Pauleit, S., Rötzer, T., 2023. Urban environment, drought events and climate change strongly affect the growth of common urban tree species in a temperate city. Urban For. Urban Green. 88, 128083 https://doi.org/10.1016/j.ufug.2023.128083.

Gill, S.E., Handley, J.F., Ennos, A.R., Pauleit, S., 2007. Adapting cities for climate change: the role of the green infrastructure. Built. Environ. 33 (1), 115–133. https://doi.org/10.2148/benv.33.1.115.

Gillner, S., Vogt, J., Tharang, A., Dettmann, S., Roloff, A., 2015. Role of street trees in mitigating effects of heat and drought at highly sealed urban sites. Landsc. Urban Plann. 143, 33–42. https://doi.org/10.1016/j.landurbplan.2015.06.005.

Gillner, S., Korn, S., Hofmann, M., Roloff, A., 2017. Contrasting strategies for tree species to cope with heat and dry conditions at urban sites. Urban Ecosyst. 20 (4), 853–865. https://doi.org/10.1007/s11252-016-0636-z.

Grueber, C.E., Nakagawa, S., Laws, R.J., Jamieson, I.G., 2011. Multimodel inference in ecology and evolution: challenges and solutions: multimodel inference. J. Evol. Biol. 24 (4), 699–711. https://doi.org/10.1111/j.1420-9101.2010.02210.x.

Heusinkveld, B.G., Steeneveld, G.J., van Hove, L.W.A., Jacobs, C.M.J., Holtslag, A.a.M., 2014. Spatial variability of the Rotterdam urban heat island as influenced by urban land use. J. Geophys. Res. Atmos. 119 (2), 677–692. https://doi.org/10.1002/2012JD019399.

Honold, M., 2021. *Influence Of Urban Environment and Climate Change on Basal Area Growth of Four Common Urban Tree Species in Munich* [Master's Thesis]. Technical University of, Munich.

Höppe, P., 1999. The physiological equivalent temperature—a universal index for the biometeorological assessment of the thermal environment. Int. J. Biometeorol. 43 (2), 71–75. https://doi.org/10.1007/s004840050118.

Iungman, T., Cirach, M., Marando, F., Pereira Barboza, E., Khomenko, S., Masselot, P., Quijal-Zamorano, M., Mueller, N., Gasparrini, A., Urquiza, J., Heris, M., Thondoo, M., Nieuwenhuijsen, M., 2023. Cooling cities through urban green infrastructure: a health impact assessment of European cities. Lancet S0140673622025855. https://doi.org/10.1016/S0140-6736(22)02585-5.

Jiao, L., Lu, N., Fu, B., Gao, G., Wang, S., Jin, T., Zhang, L., Liu, J., Zhang, D., 2016. Comparison of transpiration between different aged black locust (Robinia pseudoacacia) trees on the semi-arid Loess Plateau, China. Journal of Arid Land 8 (4), 604–617. https://doi.org/10.1007/s40333-016-0047-2.

Konarska, J., Uddling, J., Holmer, B., Lutz, M., Lindberg, F., Pleijel, H., Thorsson, S., 2016. Transpiration of urban trees and its cooling effect in a high latitude city. Int. J. Biometeorol. 60 (1), 159–172. https://doi.org/10.1007/s00484-015-1014-x.

Lahr, E.C., Dunn, R.R., Frank, S.D., 2018. Variation in photosynthesis and stomatal conductance among red maple (Acer rubrum) urban planted cultivars and wildtype trees in the southeastern United States. PLoS One 13 (5), e0197866. https://doi.org/10.1371/journal.pone.0197866.

Lee, H., Mayer, H., Chen, L., 2016. Contribution of trees and grasslands to the mitigation of human heat stress in a residential district of Freiburg, Southwest Germany. Landsc. Urban Plann. 148, 37–50. https://doi.org/10.1016/j.landurbplan.2015.12.004.

Lindén, J., Fonti, P., Esper, J., 2016. Temporal variations in microclimate cooling induced by urban trees in Mainz, Germany. Urban For. Urban Green. 20, 198–209. https://doi.org/10.1016/j.ufug.2016.09.001.

Livesley, S.J., McPherson, E.G., Calfapietra, C., 2016. The urban forest and ecosystem services: impacts on urban water, heat, and pollution cycles at the tree, street, and city scale. J. Environ. Qual. 45 (1), 119–124. https://doi.org/10.2134/jeq2015.11.0567.

Manickathan, L., Defraeye, T., Allegrini, J., Derome, D., Carmeliet, J., 2018. Parametric study of the influence of environmental factors and tree properties on the transpirative cooling effect of trees. Agric. For. Meteorol. 248, 259–274. https://doi.org/10.1016/j.agrformet.2017.10.014.

Massetti, L., Petralli, M., Napoli, M., Brandani, G., Orlandini, S., Pearlmutter, D., 2019. Effects of deciduous shade trees on surface temperature and pedestrian thermal stress during summer and autumn. Int. J. Biometeorol. 63 (4), 467–479. https://doi.org/10.1007/s00484-019-01678-1.

Matzarakis, A., Rutz, F., Mayer, H., 2010. Modelling radiation fluxes in simple and complex environments: basics of the RayMan model. Int. J. Biometeorol. 54 (2), 131–139. https://doi.org/10.1007/s00484-009-0261-0.

München, L.H., 2023. Statistische Daten zur Münchner Bevölkerung. https://stadt.muenchen.de/infos/statistik-bevoelkerung.html.

McClung, T., Ibáñez, I., 2018. Quantifying the synergistic effects of impervious surface and drought on radial tree growth. Urban Ecosyst. 21 (1), 147–155. https://doi.org/10.1007/s11252-017-0699-5.

McDonnell, M.J., Hahs, A.K., 2008. The use of gradient analysis studies in advancing our understanding of the ecology of urbanizing landscapes: current status and future directions. Landsc. Ecol. 23 (10), 1143–1155. https://doi.org/10.1007/s10980-008-9253-4.

McDonnell, M.J., Pickett, S.T.A., 1990. Ecosystem structure and function along urban-rural gradients: an unexploited opportunity for ecology. Ecology 71 (4), 1232–1237. https://doi.org/10.2307/1938259.

Moser, A., Rötzer, T., Pauleit, S., Pretzsch, H., 2016. The urban environment can modify drought stress of small-leaved lime (tilia cordata mill.) and black locust (Robinia pseudoacacia L.). Forests 7 (3). https://doi.org/10.3390/f7030071. Article 3.

Moser, A., Rahman, M.A., Pretzsch, H., Pauleit, S., Rötzer, T., 2017. Inter- and intraannual growth patterns of urban small-leaved lime (Tilia cordata mill.) at two public squares with contrasting microclimatic conditions. Int. J. Biometeorol. 61 (6), 1095–1107. https://doi.org/10.1007/s00484-016-1290-0.

Moser, A., Uhl, E., Rötzer, T., Biber, P., Caldentey, J.M., Pretzsch, H., 2018. Effects of climate trends and drought events on urban tree growth in Santiago de Chile. Ciencia e Investigación Agraria 45 (1), 35–50. https://doi.org/10.7764/rcia.v45i1.1793.

Moser-Reischl, A., Rötzer, T., Pauleit, S., Pretzsch, H., 2021. Urban tree growth characteristics of four common species in south Germany. Arboric. Urban For. 47 (4), 150–169. https://doi.org/10.48044/jauf.2021.015.

Moss, J.L., Doick, K.J., Smith, S., Shahrestani, M., 2019. Influence of evaporative cooling by urban forests on cooling demand in cities. Urban For. Urban Green. 37, 65–73. https://doi.org/10.1016/j.ufug.2018.07.023.

Niinemets, Ü., Valladares, F., 2006. Tolerance to shade, drought, and waterlogging of temperate northern hemisphere trees and shrubs. Ecol. Monogr. 76 (4), 521–547. https://doi.org/10.1890/0012-9615(2006)076[0521:TTSDAW]2.0.CO;2.

Oke, T.R., 1973. City size and the urban heat island. Atmos. Environ. 7 (8), 769–779. https://doi.org/10.1016/0004-6981(73)90140-6, 1967.

Oke, T.R., 1988. The urban energy balance. Prog. Phys. Geogr. Earth Environ. 12 (4), 471–508. https://doi.org/10.1177/030913338801200401.

Pauleit, S., Duhme, F., 2000. Assessing the environmental performance of land cover types for urban planning. Landsc. Urban Plann. 52 (1), 1–20. https://doi.org/10.1016/S0169-2046(00)00109-2.

Pauleit, S., Jones, N., Garcia-Martin, G., Garcia-Valdecantos, J.L., Rivière, L.M., Vidal-Beaudet, L., Bodson, M., Randrup, T.B., 2002. Tree establishment practice in towns and cities – results from a European survey. Urban For. Urban Green. 1 (2), 83–96. https://doi.org/10.1078/1618-8667-00009.

Pauleit, S., Liu, L., Ahern, J., Kazmierczak, A., 2011. Multifunctional green infrastructure planning to promote ecological services in the city. https://doi.org/10.1093/acprof:oso/9780199563562.003.0033.

Pauleit, S., Fryd, O., Backhaus, A., Jensen, M.B., 2020. Green infrastructures to face climate change in an urbanizing world. In: Loftness, V. (Ed.), Sustainable Built Environments. Springer US, pp. 207–234. https://doi.org/10.1007/978-1-0716-0684-1_212.

Pongracz, R., Bartholy, J., Dezso, Z., 2006. Remotely sensed thermal information applied to urban climate analysis. Adv. Space Res. 37 (12), 2191–2196. https://doi.org/10.1016/j.asr.2005.06.069.

Pretzsch, H., Biber, P., Uhl, E., Dahlhausen, J., Schütze, G., Perkins, D., Rötzer, T., Caldentey, J., Koike, T., Con, T. van, Chavanne, A., Toit, B. du, Foster, K., Lefer, B., 2017. Climate change accelerates growth of urban trees in metropolises worldwide. Sci. Rep. 7 (1) https://doi.org/10.1038/s41598-017-14831-w. Article 1.

Qiu, G.Y., Zou, Z., Li, X., Li, H., Guo, Q., Yan, C., Tan, S., 2017. Experimental studies on the effects of green space and evapotranspiration on urban heat island in a subtropical megacity in China. Habitat Int. 68, 30–42. https://doi.org/10.1016/j.habitatint.2017.07.009.

Radoglou, K., Dobrowolska, D., Spyroglou, G., Valeriu-Norocel, N., 2009. A review on the ecology and silviculture of limes: (Tilia cordata Mill., Tilia platyphyllos Scop, and Tilia tomentosa Moench.) in Europe. BODENKULTUR -WIEN AND MUNCHEN 3, 9–20.

Rahman, M.A., Armson, D., Ennos, A.R., 2015. A comparison of the growth and cooling effectiveness of five commonly planted urban tree species. Urban Ecosyst. 18 (2), 371–389. https://doi.org/10.1007/s11252-014-0407-7.

Rahman, M.A., Moser, A., Rötzer, T., Pauleit, S., 2017a. Microclimatic differences and their influence on transpirational cooling of Tilia cordata in two contrasting street canyons in Munich, Germany. Agric. For. Meteorol. 232, 443–456. https://doi.org/10.1016/j.agrformet.2016.10.006.

Rahman, M.A., Moser, A., Rötzer, T., Pauleit, S., 2017b. Within canopy temperature differences and cooling ability of Tilia cordata trees grown in urban conditions. Build. Environ. 114, 118–128. https://doi.org/10.1016/j.buildenv.2016.12.013.

Rahman, M.A., Hartmann, C., Moser-Reischl, A., von Strachwitz, M.F., Paeth, H., Pretzsch, H., Pauleit, S., Rötzer, T., 2020a. Tree cooling effects and human thermal comfort under contrasting species and sites. Agric. For. Meteorol. 287, 107947 https://doi.org/10.1016/j.agrformet.2020.107947.

Rahman, M.A., Smith, J.G., Stringer, P., Ennos, A.R., 2011. Effect of rooting conditions on the growth and cooling ability of Pyrus calleryana. Urban Forest. Urban Green. 10 (3), 185–192. https://doi.org/10.1016/j.ufug.2011.05.003.

Rahman, M.A., Stratopoulos, L.M.F., Moser-Reischl, A., Zölch, T., Häberle, K.-H., Rötzer, T., Pretzsch, H., Pauleit, S., 2020b. Traits of trees for cooling urban heat islands: a meta-analysis. Build. Environ. 170, 106606 https://doi.org/10.1016/j.buildenv.2019.106606.

Rahman, M.A., Dervishi, V., Moser-Reischl, A., Ludwig, F., Pretzsch, H., Rötzer, T., Pauleit, S., 2021. Comparative analysis of shade and underlying surfaces on cooling effect. Urban For. Urban Green. 63, 127223 https://doi.org/10.1016/j.ufug.2021.127223.

Rahman, M.A., Franceschi, E., Pattnaik, N., Moser-Reischl, A., Hartmann, C., Paeth, H., Pretzsch, H., Rötzer, T., Pauleit, S., 2022. Spatial and temporal changes of outdoor thermal stress: influence of urban land cover types. Sci. Rep. 12 (1), 671. https://doi.org/10.1038/s41598-021-04669-8.

Rahman, M.A., Arndt, S., Bravo, F., Cheung, P.K., Van Doorn, N., Franceschi, E., Del Río, M., Livesley, S.J., Moser-Reischl, A., Pattnaik, N., Rötzer, T., Paeth, H., Pauleit, S., Preisler, Y., Pretzsch, H., Tan, P.Y., Cohen, S., Szota, C., Torquato, P.R., 2024. More than a canopy cover metric: influence of canopy quality, water-use strategies and site climate on urban forest cooling potential. Landsc. Urban Plann. 248, 105089 https://doi.org/10.1016/j.landurbplan.2024.105089.

Ren, Z., Zhao, H., Fu, Y., Xiao, L., Dong, Y., 2022. Effects of urban street trees on human thermal comfort and physiological indices: a case study in Changchun city, China. J. For. Res. 33 (3), 911–922. https://doi.org/10.1007/s11676-021-01361-5.

Roloff, A., 2013. Bäume in der Stadt. Besonderheiten, Funktion, Nutzen, Arten, Risiken. Verlag Eugen Ulmer.

Rötzer, T., Rahman, M.A., Moser-Reischl, A., Pauleit, S., Pretzsch, H., 2019. Process based simulation of tree growth and ecosystem services of urban trees under present and future climate conditions. Sci. Total Environ. 676, 651–664. https://doi.org/10.1016/j.scitotenv.2019.04.235.

Rötzer, T., Moser-Reischl, A., Rahman, M.A., Hartmann, C., Paeth, H., Pauleit, S., Pretzsch, H., 2021. Urban tree growth and ecosystem services under extreme

drought. Agric. For. Meteorol. 308–309, 108532 https://doi.org/10.1016/j.agrformet.2021.108532.
Sanusi, R., Livesley, S.J., 2020. London Plane trees (Platanus x acerifolia) before, during and after a heatwave: losing leaves means less cooling benefit. Urban For. Urban Green. 54, 126746 https://doi.org/10.1016/j.ufug.2020.126746.
Schneider, C., Neuwirth, B., Schneider, S., Balanzategui, D., Elsholz, S., Fenner, D., Meier, F., Heinrich, I., 2022. Using the dendro-climatological signal of urban trees as a measure of urbanization and urban heat island. Urban Ecosyst. 25 (3), 849–865. https://doi.org/10.1007/s11252-021-01196-2.
Shashua-Bar, L., Tsiros, I.X., Hoffman, M.E., 2010. A modeling study for evaluating passive cooling scenarios in urban streets with trees. Case study: athens, Greece. Build. Environ. 45 (12), 2798–2807. https://doi.org/10.1016/j.buildenv.2010.06.008.
Shashua-Bar, L., Pearlmutter, D., Erell, E., 2011. The influence of trees and grass on outdoor thermal comfort in a hot-arid environment. Int. J. Climatol. 31 (10), 1498–1506. https://doi.org/10.1002/joc.2177.
Smithers, R.J., Doick, K.J., Burton, A., Sibille, R., Steinbach, D., Harris, R., Groves, L., Blicharska, M., 2018. Comparing the relative abilities of tree species to cool the urban environment. Urban Ecosyst. 21 (5), 851–862. https://doi.org/10.1007/s11252-018-0761-y.
Taha, H., 1997. Urban climates and heat islands: albedo, evapotranspiration, and anthropogenic heat. Energy Build. 25 (2), 99–103. https://doi.org/10.1016/S0378-7788(96)00999-1.
Taubenböck, H., Reiter, M., Dosch, F., Leichtle, T., Weigand, M., Wurm, M., 2021. Which city is the greenest? A multi-dimensional deconstruction of city rankings. Comput. Environ. Urban Syst. 89, 101687 https://doi.org/10.1016/j.compenvurbsys.2021.101687.
Thorsson, S., Lindberg, F., Eliasson, I., Holmer, B., 2007. Different methods for estimating the mean radiant temperature in an outdoor urban setting. Int. J. Climatol. 27 (14), 1983–1993. https://doi.org/10.1002/joc.1537.
Wang, H., Ouyang, Z., Chen, W., Wang, X., Zheng, H., Ren, Y., 2011. Water, heat, and airborne pollutants effects on transpiration of urban trees. Environmental Pollution 159 (8), 2127–2137. https://doi.org/10.1016/j.envpol.2011.02.031.
Wang, J., Zhou, W., Jiao, M., Zheng, Z., Ren, T., Zhang, Q., 2020. Significant effects of ecological context on urban trees' cooling efficiency. ISPRS J. Photogrammetry Remote Sens. 159, 78–89. https://doi.org/10.1016/j.isprsjprs.2019.11.001.
Wang, J., Zhou, W., Jiao, M., 2022. Location matters: planting urban trees in the right places improves cooling. Front. Ecol. Environ. 20 (3), 147–151. https://doi.org/10.1002/fee.2455.
Wang, X., Rahman, M.A., Mokroš, M., Rötzer, T., Pattnaik, N., Pang, Y., Zhang, Y., Da, L., Song, K., 2023. The influence of vertical canopy structure on the cooling and humidifying urban microclimate during hot summer days. Landsc. Urban Plann. 238, 104841 https://doi.org/10.1016/j.landurbplan.2023.104841.
Winbourne, J.B., Jones, T.S., Garvey, S.M., Harrison, J.L., Wang, L., Li, D., Templer, P.H., Hutyra, L.R., 2020. Tree transpiration and urban temperatures: current understanding, implications, and future research directions. Bioscience 70 (7), 576–588. https://doi.org/10.1093/biosci/biaa055.
Zimmermann, J., Link, R.M., Hauck, M., Leuschner, C., Schuldt, B., 2021. 60-year record of stem xylem anatomy and related hydraulic modification under increased summer drought in ring- and diffuse-porous temperate broad-leaved tree species. Trees (Berl.) 35 (3), 919–937. https://doi.org/10.1007/s00468-021-02090-2.
Ziter, C.D., Pedersen, E.J., Kucharik, C.J., Turner, M.G., 2019. Scale-dependent interactions between tree canopy cover and impervious surfaces reduce daytime urban heat during summer. Proc. Natl. Acad. Sci. USA 116 (15), 7575–7580. https://doi.org/10.1073/pnas.1817561116.
Zölch, T., Maderspacher, J., Wamsler, C., Pauleit, S., 2016. Using green infrastructure for urban climate-proofing: an evaluation of heat mitigation measures at the micro-scale. Urban For. Urban Green. 20, 305–316. https://doi.org/10.1016/j.ufug.2016.09.011.
Zuur, A.F., Ieno, E.N., Chris, S. Elphick, 2010. A protocol for data exploration to avoid common statistical problems. Methods Ecol. Evol. 1 (1), 3–14. https://doi.org/10.1111/j.2041-210X.2009.00001.x.